

See discussions, stats, and author profiles for this publication at: <https://www.researchgate.net/publication/325739236>

Tribological characterisation of epoxy–graphene–liquid filler composite coatings on steel under base oil external lubrication

Article in Tribology - Materials Surfaces & Interfaces · June 2018

DOI: 10.1080/17515831.2018.1482719

CITATIONS

8

READS

261

3 authors, including:



Vikram Kumar

Indian Institute of Technology Kanpur

46 PUBLICATIONS 757 CITATIONS

[SEE PROFILE](#)



Avinash Kumar Agarwal

Indian Institute of Technology Kanpur

582 PUBLICATIONS 23,261 CITATIONS

[SEE PROFILE](#)



Tribological characterisation of epoxy–graphene–liquid filler composite coatings on steel under base oil external lubrication

Vikram Kumar, Sujeet K. Sinha & Avinash K. Agarwal

To cite this article: Vikram Kumar, Sujeet K. Sinha & Avinash K. Agarwal (2018): Tribological characterisation of epoxy–graphene–liquid filler composite coatings on steel under base oil external lubrication, Tribology - Materials, Surfaces & Interfaces, DOI: [10.1080/17515831.2018.1482719](https://doi.org/10.1080/17515831.2018.1482719)

To link to this article: <https://doi.org/10.1080/17515831.2018.1482719>



Published online: 12 Jun 2018.



Submit your article to this journal [↗](#)



View related articles [↗](#)



View Crossmark data [↗](#)



Tribological characterisation of epoxy–graphene–liquid filler composite coatings on steel under base oil external lubrication

Vikram Kumar, Sujeet K. Sinha and Avinash K. Agarwal

Indian Institute of Technology Delhi, New Delhi, India

ABSTRACT

In our earlier study, epoxy-based composites with graphene (10 wt-%) and *in situ* liquid fillers (base oil SN150 or perfluoropolyether at 10 wt-%) were found to provide low friction and highly wear durable as thin coatings on the steel substrate in dry interfacial state. In this present work, we have tested this composite in the presence of an external lubricant (base oil SN150). The lowest coefficient of friction was recorded as 0.04 and the lowest specific wear rate was measured as $9.8 \times 10^{-7} \text{ mm}^3 \text{ Nm}^{-1}$ for the composites without any failure of the coating up to 200,000 sliding cycles. It is shown that such polymeric coatings can be an excellent boundary film in both dry and lubricated conditions for various bearings.

ARTICLE HISTORY

Received 6 October 2017
Accepted 24 May 2018

KEYWORDS

Epoxy; Graphene; Liquid filler; Polymer composite coating

Introduction

The tribological performances of machine parts, such as gears, bearings, engine piston rings, etc. can be drastically improved by applying a suitable coating on both or one of the mating surfaces [1]. Several hard and soft tribological coatings have been developed in the past according to the stress and thermal requirements at the interface. Among hard coatings, diamond-like-carbon (DLC), WC, TiC, TiAlN, CrC, etc. [2–6] have been successfully used for tribological applications. Hard coatings are also suitable for machine tools where hardness, wear resistance and thermal resistance are the main requirements. Some of the drawbacks of hard coatings are that they provide high friction (exceptions are DLC, MoS₂, etc.), high interfacial stress between the substrate and the coating, poor adhesion to the substrate [7], high wear against itself or a harder material, abrasive to the counterface and non-reactivity to the lubricant molecules [8]. In addition, most of the hard coatings tend to be very brittle, and hence once a defect (crack) initiates, it grows at a fast rate leading to its complete delamination from the substrate. The delaminated wear debris of hard coating material (or, the third body) is very damaging to both the interacting surfaces which quickly increases the wear of both surfaces. In order to mitigate the above, several researchers have experimented with softer polymeric coatings. Polymers can have better adhesion to the substrate, low friction and are not damaging to the counterface [9,10]. Epoxy-based coatings/bulks with various fillers such as carbon materials (graphite, graphene and carbon nano tubes) [11], functionalised reduced graphene oxide [12], carbon fibre [13] and liquid lubricants (PFPE and SN150) (added *in situ*) [14,15] have shown

promising results in dry state (no external lubricant present). Polymer coatings provide low cost and environment-friendly solution to the problem of wear in machines. The liquid lubricant-filled epoxy (*in situ* lubrication) gives low friction coefficient of 0.07 for a sustained period of more than 2×10^5 number of cycle at contact stress value of 0.025 GPa and sliding speed of 0.63 m s⁻¹ [14,15].

In continuation of the previous work [15], in the present paper, the *in situ* lubricated composition of epoxy with graphene and liquid lubricants (SN150 or PFPE) were tested for tribological performances in base oil (SN150) external lubrication. This study investigated the tribology of these novel composites in sliding condition and in the presence of an external lubricant, which is the case with most machines. Base oil (SN150) (without any additive) was selected as an environmentally friendly external lubricant.

Experimental procedure

Materials

Cylindrical shafts (diameter = 40 mm) of D2 steel (composition: C = 1.4–1.6%, Cr = 11–13%, Co = 1, Mn = 0.6%, Mo = 0.7–1.2% P = 0.03% and Fe = 83.6–86%) of hardness ~58 HRC were coated with epoxy and its composites [15]. The coating thickness was ~50–60 μm. The external lubricating oil used was SN150 of Group-I with a viscosity of 24.25 cP (at 40°C). Graphene of particle sizes <100 nm was purchased from R N V Private Limited, India. Epoxy (product ID: Araldite AY 103) with hardener (product ID: HY 951) was used as the matrix (supplied by

H. A. M. Pvt. Ltd). The counterface was 4 mm diameter steel ball (SAE 52100) (hardness = 58 HRC and roughness $R_a = 50$ nm). The base oil SN150 was provided by the Indian Oil Corporation, Faridabad, India.

Test sample preparation

D2 steel was used to prepare cylindrical specimens of diameter ~ 40 mm, width ~ 12 mm and roughness $R_a \sim 0.40$ μm . Before the application of the coating, the surface was thoroughly cleaned with acetone. The substrate was air-dried and cleaned by air plasma treatment. This surface treatment removes organic impurities and generates carboxyl groups on the substrate and increases the adhesion of the coatings with the substrate [11]. Four compositions of the coating were prepared (Table 1). The method of application of the coating on the steel shaft substrate and curing procedure was explained in our earlier work [15]. The final thickness of the coating after curing varied from ~ 50 – 60 μm .

Mechanical (tensile and hardness) and thermal properties of epoxy and its composites

Mechanical properties

Tensile strength, elastic modulus and hardness of epoxy and the composites were measured. The tensile test was used for the bulk material and Vickers hardness test was used for measuring coating properties. The data were provided in our previous paper for pure epoxy (EP), epoxy + 10 wt-% graphene (EGN), Epoxy + 10 wt-% Graphene + 10 wt-% SN150 (EGNSN) and Epoxy + 10 wt-% Graphene + 10 wt-% PFPE (EGNPFPE) specimens.

From the tensile test data, it was seen that adding graphene or graphene with liquid filler (SN150) increased the tensile strength by ~ 20 and $\sim 10\%$, respectively, of the bulk epoxy. One of the reasons for this enhancement could be because the graphene particles providing more surface area for bonding during curing and thus strengthening it. Adding PFPE keeps the tensile strength in the same range as that of pure epoxy. It is possible that the lubricant molecules (PFPE) compromise the bonding of epoxy with graphene. The total (elastic and plastic) % elongation at failure of pure epoxy was 14% which reduced to 9% for EGN, to 7.7% for EGNSN and to 7% for EGNPFPE. Increased brittleness of the composites will lead to crack sensitivity in tensile loading.

Table 1. Different type of coating composition and their nomenclature.

Composition	Nomenclature used
Epoxy	EP
Epoxy + 10 wt-% Graphene	EGN
Epoxy + 10 wt-% Graphene + 10 wt-% SN150	EGNSN
Epoxy + 10 wt-% Graphene + 10 wt-% PFPE	EGNPFPE

Table 2. The percentage plastic elongation of epoxy and its composites obtained from the tensile test data.

Composite	Yield stress MPa	Rupture strain	Yield strain	Plastic elongation (%)
EP	45.21	0.145	0.082	6.36
EGN	47.61	0.094	0.075	1.99
EGNSN	45.38	0.077	0.076	0.12
EGNPFPE	39.32	0.075	0.072	0.27

The data show that the composites undergo much less plastic deformation before failure in comparison to that of pure epoxy.

Plastic elongation (%) was obtained by measuring the yield strain and rupture strain in the tensile test. The % plastic deformation is presented in Table 2 which were calculated by the formula as given below,

$$\% \text{Plastic Elongation} = (\text{Rupture Strain} - \text{Yield Strain}) \times 100$$

The data show that the composites undergo much less plastic deformation before failure in comparison to that of pure epoxy.

Hardness data were presented in Ref. [15]. An important observation was that hardness values for EGNSN and EGNPFPE composite samples were somewhat lower than that of pure epoxy. It is believed that the presence of *in situ* lubricant on the surface of specimen helps in the penetration of an indenter into the material. Hence, the calculated hardness for composites with lubricant filler is low.

Thermogravimetry

Thermal stability of epoxy and epoxy composites were estimated using high-temperature simultaneous Thermo Gravimetric Analyzer (TGA) and Differential Scanning Calorimetry (DSC) (STA 800 Perkin Elmer Ltd.). With the TGA, thermal decomposition temperatures of materials were investigated. The heating rate was $10^\circ\text{C min}^{-1}$ from 30 to 600°C then holding for 5 min at 600°C followed by cooling at the rate of $30^\circ\text{C min}^{-1}$ from 600 to 30°C . DSC analysis was also carried out with the same temperature parameters as TGA, which gave the plot of differential heat as a function of temperature. Any peak in the plot showed the transformation of material. Thus from Figure 1(a and b), the decomposition temperatures for pure epoxy and epoxy composites were found to be $\sim 328^\circ\text{C}$. It proves that the composites are thermally as stable as pure epoxy despite the addition of liquid lubricants. Hence, these composites are suitable for use in high-temperature applications such as engine piston rings.

Tribological test

Tribological (friction and wear) performances were investigated using a lubricant tribo-tester (ball-on-cylinder geometry) as shown in our previous

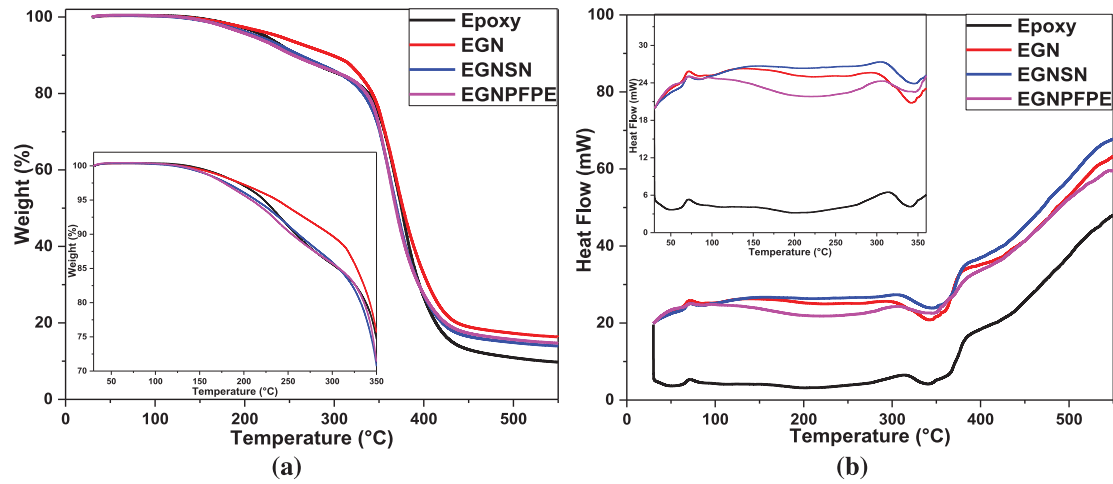


Figure 1. (a) TGA and (b) DSC thermograms for epoxy and its composites.

publication [11]. A schematic of the tester is presented in the Supplementary Data as Figure S1. The cylindrical outer surface of D2 steel was coated with epoxy or its composites. The counterface used was 4 mm diameter bearing steel (SAE 52100) ball. The normal load used was 10 N. The linear speed at the surface of the coating was varied from 0.021 to 2.09 m s⁻¹. The initial coefficient of friction (CoF) was evaluated by averaging first 500 cycles whereas the steady-state CoF was evaluated by averaging 1000 cycles before failure. The tests were also carried out at three different loads (3, 6 and 10 N) and a fixed sliding speed of 0.63 m s⁻¹ to investigate the load effects. The ambient room temperature and relative humidity were 25 ± 2°C and 45 ± 5%, respectively. Each test was repeated three times and averages of the three data with standard deviations were used for plotting and analysis. Stribeck curve was also plotted for the epoxy composites. For this curve, the CoF was plotted against Sommerfeld number ($\eta V/P$), where η is the viscosity of the lubricant, V is the sliding speed and P is the apparent contact pressure. The wear track width and depth profile were measured by the 3D optical profiler. The volumetric wear rate was computed by dividing the wear volume with the normal load multiplied by the sliding distance (mm³Nm⁻¹). Worn track created on the cylindrical specimen and wear scar on the ball surface were captured by the confocal microscope.

Surface characterisation of epoxy and composites

Surface roughness

The roughness of neat epoxy and composite coatings on cylindrical specimen were measured using the Surface Roughness Analyzer (SurfTest SJ-301, Mitutoyo) at a minimum of five points and average value with standard deviation are reported in Table 3. The

Table 3. Surface roughness of pure epoxy and epoxy composites coating.

Coating	EP	EGN	EGNSN	EGNPFPE
Roughness R_a (μm)	0.126 ± .004	0.176 ± .004	0.373 ± .021	0.43 ± .053

pure epoxy coating was very smooth and the roughness increased 2–3 times for the composites. It was observed that liquid-filled composites gave very high roughness because of the globular pockets of the liquid droplets, which were exposed on the top surface of the coating.

Contact angle of coating surfaces

Oil (SN150) and water contact angles of epoxy and composite coatings on the steel cylindrical specimen were measured by Goniometer (optical contact angle, Data Physics) and the data are presented in Table 4. With water, there is no change in the surface reactivity after adding graphene and the lubricants. The epoxy and epoxy composite surfaces remain in the hydrophilic range. With oil contact angle, there is a tendency for the composite (EGN) to become oleophilic after adding graphene. It is because of greater affinity of SN150 with graphene. It can practically help in building a thin fluid film at the interface during external lubrication. For the composite with SN150 (EGNSN), the oil contact angle remains low because of the cohesive interaction between the oil present in the composite *in situ* and the oil droplet during the measurement. For the composite with PFPE (EGNPFPE), the oil contact angle increases

Table 4. Water and oil contact angles of pure epoxy and epoxy composite coatings.

Coating	EP	EGN	EGNSN	EGNPFPE
Water contact angle	87.9 ± 0.1°	87.5 ± 1.0°	87.9 ± 1.6°	85 ± 0.1°
Oil (SN150) Contact angle	40 ± 0.4°	37.9 ± 2.1°	32.2 ± 0.8°	40.9 ± 2.2°

because of lesser interactions between the PFPE liquid present in the composite *in situ* and the SN150 oil droplet.

Scratch test

A conical diamond indenter with a tip radius of $100\ \mu\text{m}$ was used to perform scratch tests on each sample to estimate the adhesive bonding between the coating and the substrate and the load-bearing capacity. The scratch tests were performed at two different loads (30 and 50 mN) with a scratch velocity of $1\ \text{mm}\ \text{min}^{-1}$ for a scratch distance of 1 mm. Figure 2(a–d) are the plots of penetration depth and acoustic emission with scratch length. Graphs showed that there were no or negligible acoustic emissions which suggested no failure of coating/bonding with the substrate. Also, penetration depth was nearly zero at 30 mN load for all the coatings in the range of 250–320 nm at 50 mN load. Higher penetration depth can lead to high scratch force and associated stick–slip effect. The stick–slip event leads to greater acoustic emission output as the strain energy is stored during ‘stick’ and released during the ‘slip’ event. Energy Dispersive Spectroscopy (EDS) tests were also conducted on the gold plated samples

in order to evaluate the constituent elements present on the surfaces of the scratched polymer coating.

FTIR characterisation

Fourier transform infrared (FTIR) analyses (Thermo Scientific Nicolet 8700 Research) of EP, EGN, EGNSN and EGNPFPE composites were conducted for studying the chemical bonds and functional groups [11]. Figure 3 shows the spectra. Presence of OH group at wave number ranging from $\sim 3416\text{--}3426\ \text{cm}^{-1}$ is detected due to the presence of H_2O molecules on the surface of epoxy and its composites. There is epoxide deformation bid which contains a range of wave number $\sim 1576\text{--}1631\ \text{cm}^{-1}$, aromatic content at wave numbers 3000–3100, 1590, 1490, 830 cm^{-1} and $-\text{CH}_2$ wave number 2927 cm^{-1} . Another range of wave number 1607–559 cm^{-1} indicates epoxide deformation bid which contains aromatic, C=C, C=O, O–C, C–OH and C–O–C bonds. All composites except EGNPFPE, have similar bonding and the presence of functional group with only variation in the percentage transmittance i.e. peaks. EGNPFPE composite shows (Figure 3) less transmittance (more absorbance) compared to other composites due to the presence of C–F at wave number of 1200 cm^{-1} .

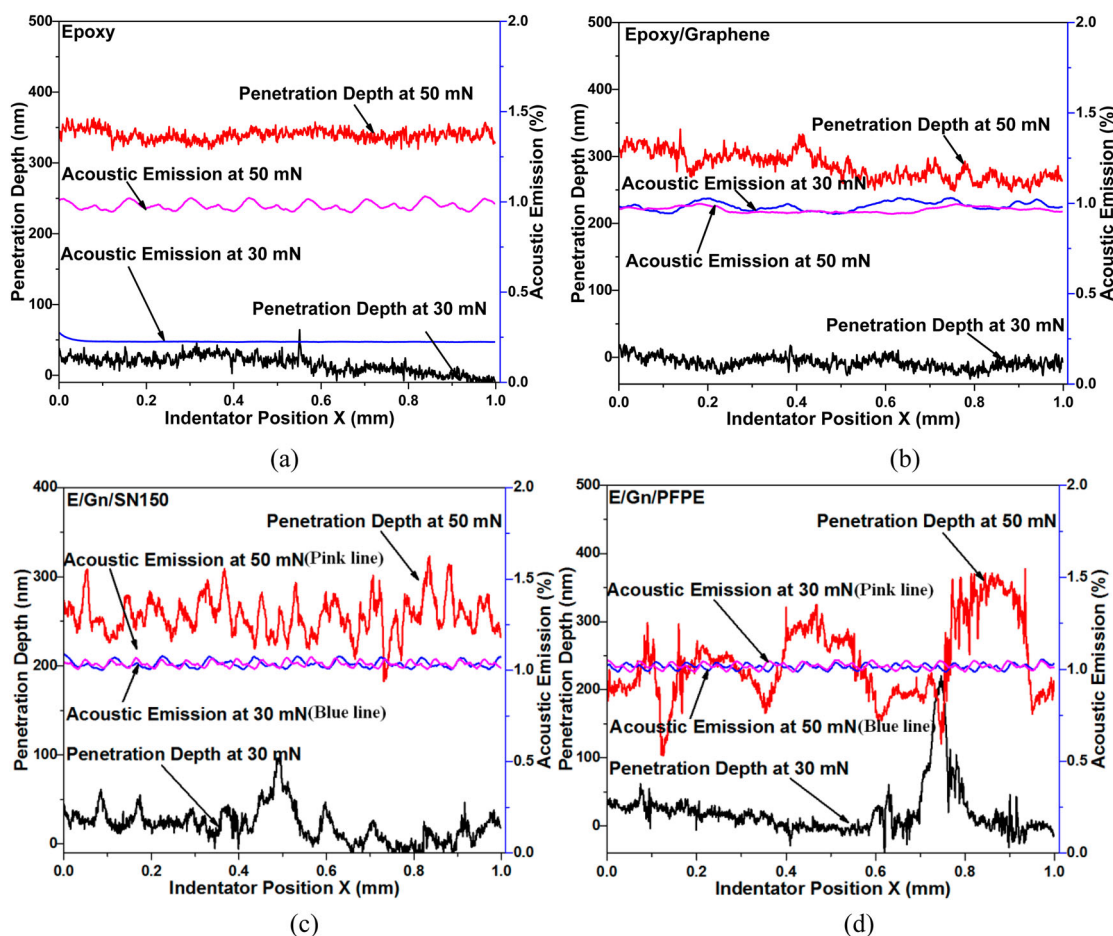


Figure 2. Acoustic emission and scratch penetration depth with scratch length for (a) EP, (b) EGN, (c) EGNSN and (d) EGNPFPE. Pristine epoxy and its composites have negligible acoustic emission and penetration depth increases as normal load is increased.

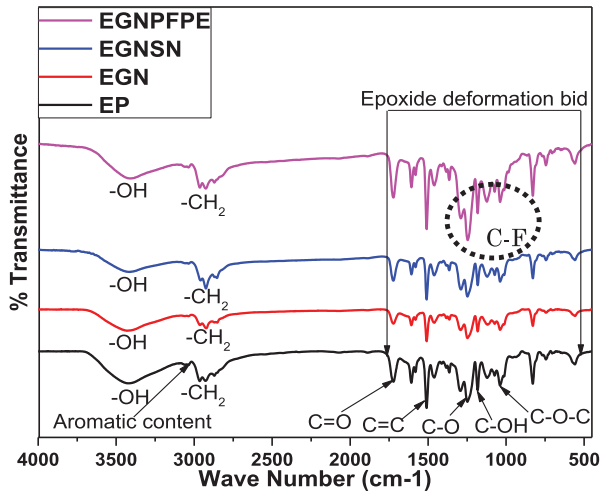


Figure 3. FTIR spectra of EP, EGN, EGNSN and EGNPFPE composites. Presence of functional groups and bonding are shown in the figure.

XPS characterisation

Figure 4 shows X-ray photoelectron spectroscopy (XPS) characterisation of EP, EGN, EGNSN and EGNPFPE samples and the atomic percentages are shown on the right side of the graph. The atomic percentages are in the form of C1s, F1s and O1s scan of epoxy and its composites. Binding energy spectra of C1s, F1s and O1s may contain the bonding of C-C, C-H, C=C, C-O, C-F, CF₂CF₂ and C=O, and O-H.

XRD pattern analysis

X-ray diffraction (XRD) patterning was conducted using D8 advance powder XRD instrument (supplied by Bruker USA) of EP, EGN, EGNSN and EGNPFPE. Bragg's Law conditions of d-spacing were satisfied by every polycrystalline material. The nature of sample

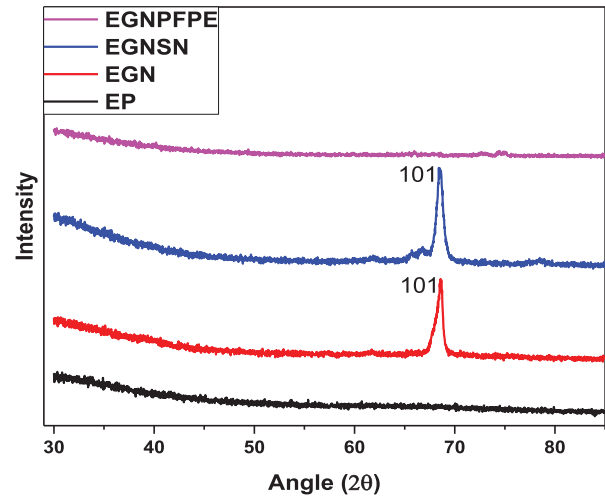


Figure 5. XRD pattern analyses of EP, EGN, EGNSN and EGNPFPE composites which exhibit the nature of crystallinity.

is identified by peak intensities of plot between angular positions and diffracted intensity. Figure 5 exhibits basal reflection (101) peak for the EGN and EGNSN at $2\theta = 68.5^\circ$ with an interlayer spacing of 0.214 nm (Bragg's law) which is due to bonding of a graphene sheet with other graphene sheet due to resin curing and the addition of base oil SN150. No peak was observed for pristine epoxy (EP) and epoxy/graphene/PFPE (EGNPFPE).

Scanning electron microscopy of coating cross-sections

Field Emission Scanning Electron Microscopy (FESEM) of cross-sections of epoxy and its composite coating were carried out using Field Emission Scanning Electron Microscope (EIGMA, Zeiss, USA) after gold coating the specimens [11]. SEM images of the cross-

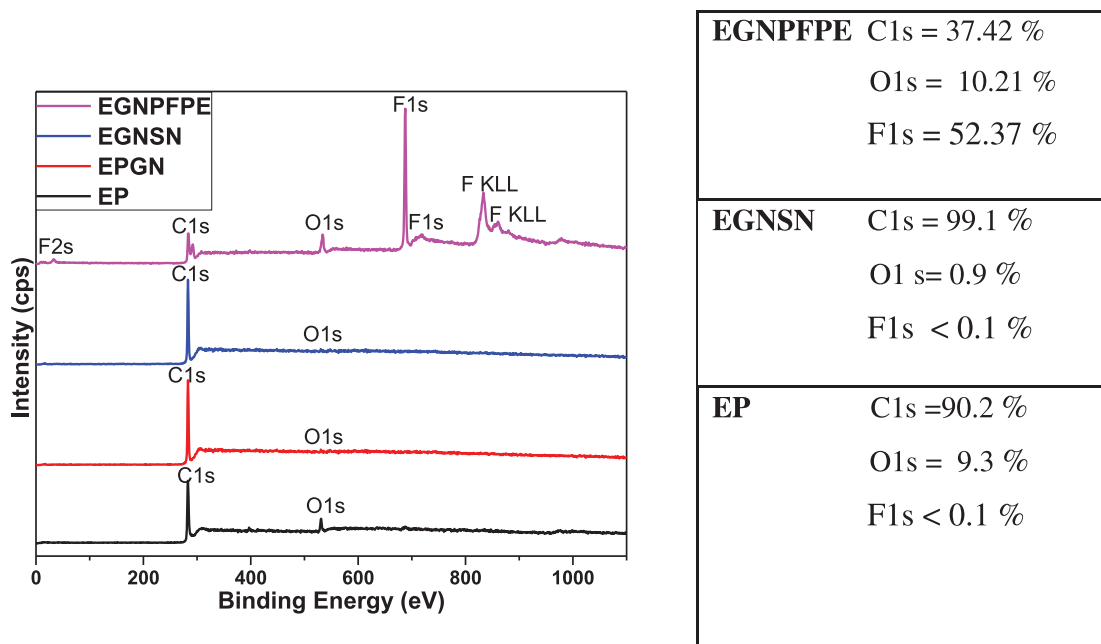


Figure 4. XPS spectra of EP, EGN, EGNSN and EGNPFPE composites showing the presence of elements and their bonding nature.

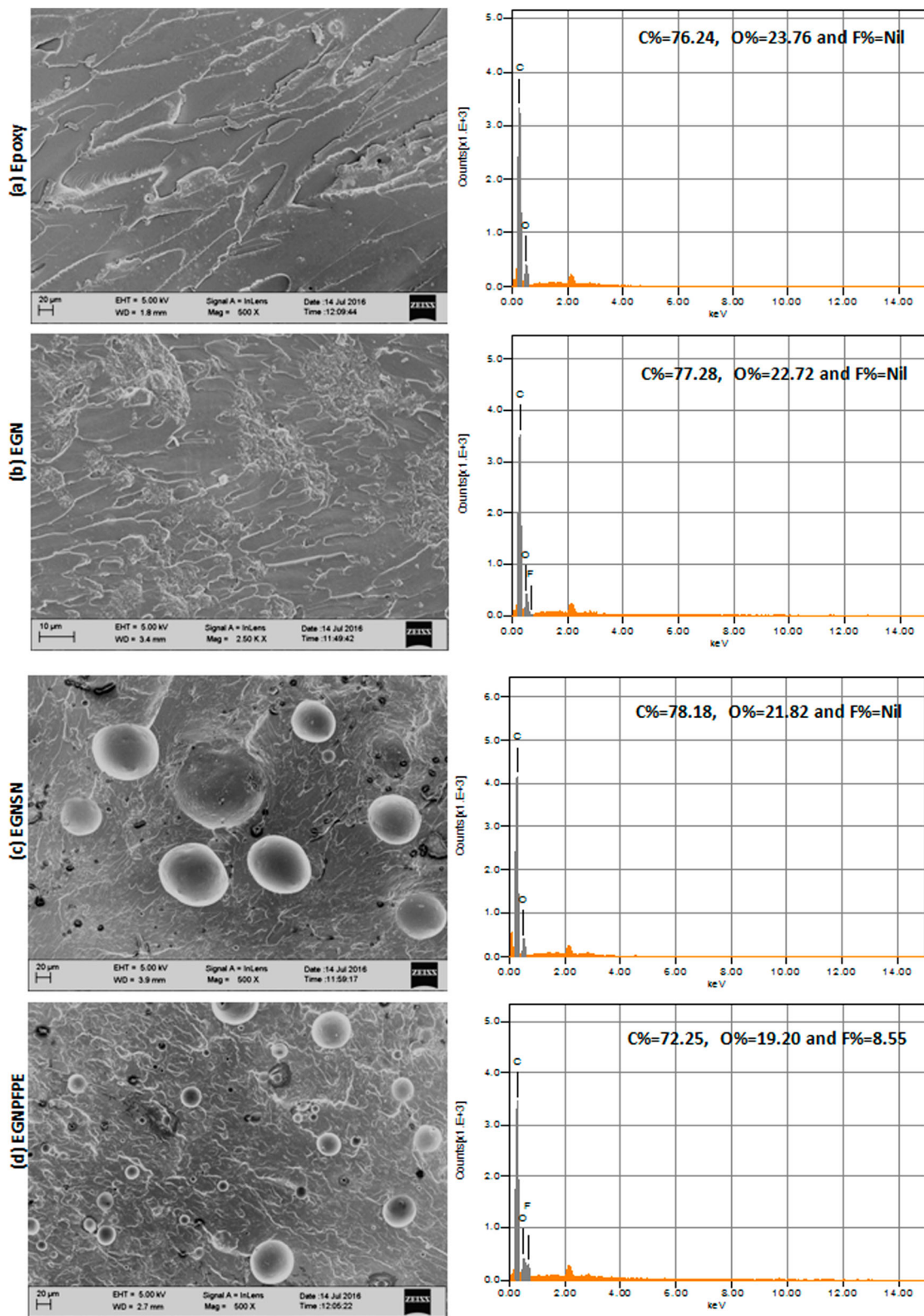


Figure 6. FESEM and EDS images of cross-section of epoxy and its composites, (a) EP, (b) EGN, (c) EGNSN and (d) EGNPFPE. The average droplet sizes of liquid lubricant distributed in composites are 50 and 20 μm of SN150 and PFPE, respectively. Graph on the right side of each FESEM image shows the EDS plots for major elements in the material.

sections of pure epoxy and composites EGN, EGNSN and EGNPFPE, are shown in Figure 6. The EDS of the cross-sections of pure epoxy and its composites were also performed using FESEM, which gives the distribution of constituent atoms in weight percentages. The distribution of liquid filler materials is seen in these cross-section images of epoxy and its composites

(Figure 6(c and d)). This clarifies that the volume of SN150 was greater than that of PFPE in the bulk epoxy. This difference in volume was because SN150 was nearly half in density to that of PFPE (density of SN150 = 840 kg m^{-3} , PFPE = 1810 kg m^{-3}). Hence, for the same wt-% of SN150 and PFPE, the volume of SN150 was nearly double. This had a positive

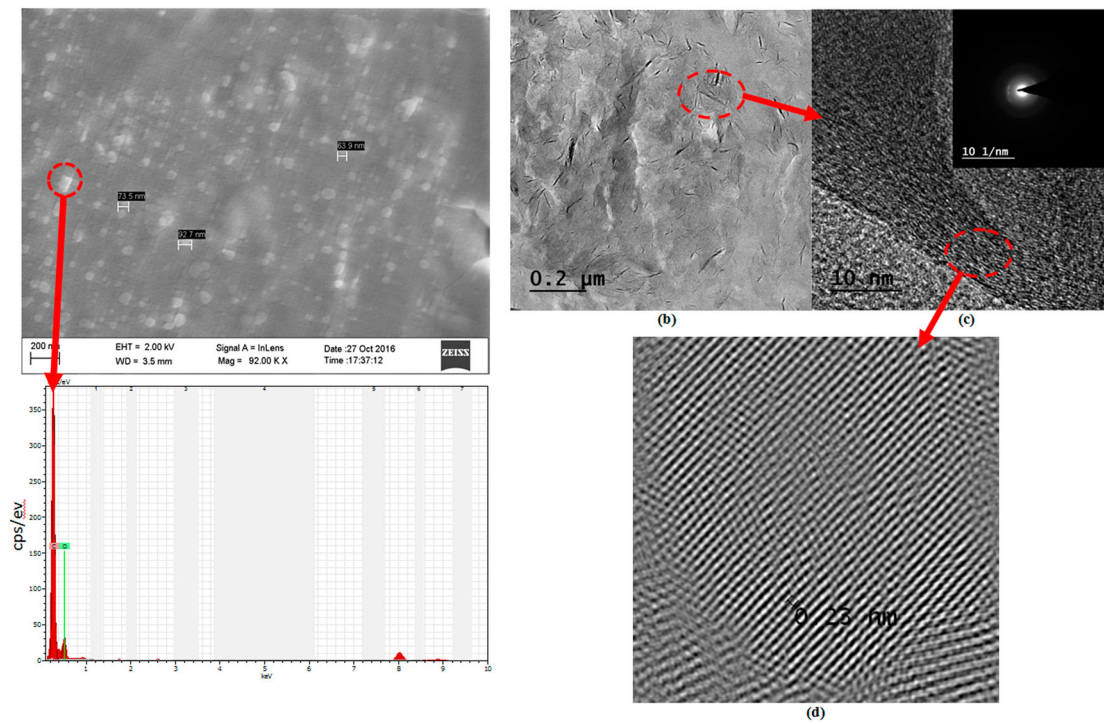


Figure 7. TEM micrograph of EGN (10 wt-%) composite showing (a) and (b) uniform distribution of graphene nanoparticles in epoxy, (c) and (d) HR TEM image of graphene particle and circular part represent the fringe pattern and confirm the presence of graphene in the composite.

effect on the reduction of the COF. Graphene distribution with SN150 was more homogeneous as compared to others due to better oleophilic nature of graphene with SN150 as seen in the oil contact angle study.

Transmission electron microscopy

Graphene particle distribution in EGN composites were investigated by TEM. Ultra-micro-toming of EGN samples was carried out by cutting a slice of nearly 100 nm thickness. High-resolution transmission electron microscopy (HR TEM) (FEI Titan G2 60–300 TEM) was used for these experiments. TEM images of EGN composite were taken (Figure 7b). The dark lines represent graphene flakes which were confirmed by HR-TEM (Figure 7c and d) measuring the lattice distance of 0.23 nm, which confirms the presence of graphene. The carbon elemental wt-% is 99.02 and oxygen elemental wt-% is 0.98 (Table 5).

Results and discussion

Stribeck curve and lubrication regimes

Stribeck curve (COF vs. Sommerfeld number) was plotted for the composites externally lubricated with base oil at 10 N normal load.¹ A normal load of 10 N for EGNSN and EGNPFPE coatings would experience the Hertzian maximum stress of 45.9 and 50.7 MPa

Table 5. Elemental analysis of EGN composite by EDS at encircled position of SEM image (Figure 7(b)) was taken and carbon, oxygen elemental wt-% are provided.

Element	Weight %	Atom %
Carbon	99.02	99.26
Oxygen	0.98	0.74

against a steel ball in dry contact condition. The Stribeck curve indicates the lubrication regimes and the mechanism at the interface. From Figure 8, at low Sommerfeld numbers (0.51–5.15), the COF first decreases and then increases, and after that, there is a very slight reduction as the Sommerfeld number is increased.

Although the COF drops in the beginning of the Stribeck curve, the minimum value of COF is 0.07 which does not indicate that the lubrication mechanism transits into hydrodynamics lubrication; i.e. the lubrication regime is of mixed type. The COF immediately rises to a higher value of 0.10 and remains in this range for both EGN and EGNSN specimens but EGNPFPE composite coating shows higher coefficient friction (0.13) with similar trend of fall and rise. The coefficients of friction of EGN and EGNSN against the same bearing steel ball without the external lubrication were found to be 0.18 and 0.09, respectively, in our previous study [15]. Hence we see that with external base lubricant, the COF is nearly comparable to the value in dry sliding condition for EGNSN. The

¹A normal load of 10 N for EGNSN and EGNPFPE coatings would impose Hertzian maximum stress of 45.9 MPa and 50.7 MPa against a steel ball (4 mm diameter) in dry contact condition. Elastic moduli of steel, EGNSN coating and EGNPFPE are taken as 200 GPa, 0.716 GPa and 0.832 GPa.

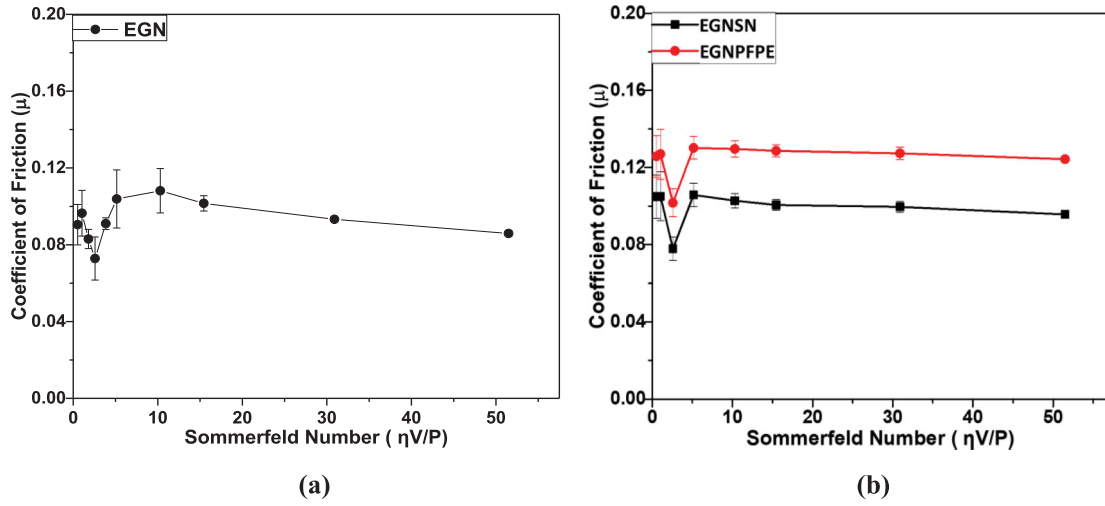


Figure 8. The COF versus Sommerfeld number for (a) EGN and (b) EGN and EGNPFPE composites in the presence of externally provided SN150 base lubricant. The normal load was 10 N and the total number of sliding cycles was 5000.

composite EGN (without *in situ* lubricant), however, shows much lower COF in the range of 0.07 with external lubricant when compared with 0.18 in dry state. This shows that the presence of *in situ* lubricant is greatly helpful in reducing the COF both in the dry and externally lubricated interfacial conditions.

Lubrication mechanism

The sliding test lubrication mechanism (Figure 9) of epoxy and its composite coatings under base oil lubrication condition could be considered as the case of boundary to mixed lubrication regimes. The frictional force for boundary lubrication mechanism is given by the following equation [16],

$$F_r = A\alpha S + (1 - \alpha)S_l \quad (1)$$

where A is the area of contacting junction and lubricant film which supports the load, α is the fraction of area

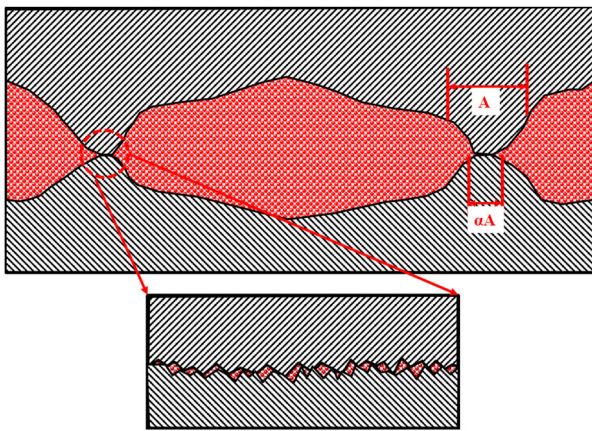


Figure 9. Schematic showing the lubrication mechanism with pure epoxy and epoxy composites coated surfaces during tribological test under base oil lubrication. The pressure over the area A was higher which contributed to load bearing and smaller area aA was asperity contact which bears the major load. There is very thin film of lubricant between the asperities as shown in enlarge image of asperity contact.

over which contacting junction is formed between the solids, S is the shear strength of solid interface and S_l is the shear strength of the liquid. For complete solid interaction, as in boundary lubrication case, α is 1 which means the frictional force is equal to the product of the real contact area and S . For complete liquid film lubrication, as in the case of hydrodynamic lubrication, $\alpha = 0$ which means the frictional force is decided by the shear strength of the liquid and the prevailing contact area. Hence, we can say that for mixed lubrication $0 < \alpha < 1$.

Under mixed lubrication regime, the total frictional force, F_T , is given by the following equation [17,18],

$$F_T = F_C + F_H \quad (2)$$

where F_C is the friction force between the (solid-solid) contacting asperities and F_H is the shear stress generated in the liquid at the prevailing shear rate and temperature (liquid film approach). Thus, the total friction force is the sum of the interacting asperities and liquid shear components.

Taking the Newtonian behaviour of lubricant liquid as a first-order approximation, the shear stress is given by the following equation:

$$\tau_H = \frac{\eta u_{\text{sliding}}}{h} \quad (3)$$

where τ_H is the shear stress, η is the viscosity of the fluid, u_{sliding} is the sliding speed and h is the film thickness. If we assume complete fluid film formation then, $\tau_H = F_T/A$, and then we can obtain the film thickness h using Equation (3). τ_H is obtained experimentally as the ratio of friction force to the real contact area (Hertzian contact). If λ is the mean asperity height of the surfaces then the ratio h/λ can be obtained. For $h/\lambda < 1$, it will be mixed lubrication case. From Table 6, we observe that the ratio h/λ is far less than 1 and hence the interface represents mixed lubrication regime.

Table 6. Contact stress, film thickness, mean asperity height and film thickness to asperity height ratio are presented in this Table.

Composite	Contact stress (τ) MPa	Mean asperity height (λ) μm	Film thickness (h) nm	Ratio (h/λ)
EP	0.345	0.225	0.442	0.00197
EGN	0.356	0.274	0.429	0.00156
EGNSN	0.532	0.885	0.287	0.00032
EGNPFPE	0.613	0.837	0.249	0.00030

As the ratio is less than one (<1), it confirms that the lubrication is in the mixed regime.

For the mixed lubrication regime, a model was proposed based on Briscoe and Evan's equation [19], which stated that the shear stress (τ) was a linear function of $\ln(V)$ [14,15], where V is the sliding velocity [14].

$$\tau = \tau_1 + \theta \ln V \quad (4)$$

where τ_1 is the shear yield stress for the initiation of sliding and θ is a coefficient. There is a good fit of the data of epoxy and its composites to Equation (4) (Figure provided in the Supplementary Data, Figure S2), which indicates that the lubrication mechanism is that of mixed lubrication. The values of τ_1 and θ are provided in the figure.

Effects of load on the CoF (with external lubrication)

The variations of initial and steady-state CoF with normal load (3, 6 and 10 N) at the linear sliding speed of 0.63 m s^{-1} (300 rev min^{-1}) are presented in Figure 10(a and b). These experiments were conducted with external lubricant (base oil SN150). The initial CoF was largely constant (within the range of 0.04–0.07) for pure EP and EGN composite at all loads (3, 6 and 10 N). However, the initial CoF increased with increasing load for EGNSN (from 0.06 to 0.09) and EGN/PFPE (from 0.07 to 0.09)

composites. The minimum initial CoF is 0.04 for EGNSN at 6 N load. It indicates that the hydrodynamic contribution (or fluid film lubrication) to the CoF is higher at low loads and the contact becomes purely asperity (solid-solid) contact when the load is increased. The steady-state CoF for EP and EGN composite were ~ 0.08 at all loads. However, steady-state CoF for EGNSN was lower (0.07) at lower loads (3 and 6 N) and increased to approximately 0.12 at 10 N load. For EGNPFPE composite, the steady-state CoF rose from 0.09 at 3 N, to 0.12 at 6 N, and to 0.14 at 10 N. It is observed from the data trends that the initial and steady-state coefficients of friction of epoxy composites filled with liquid lubricant shows higher value than those of pure EP and EGN composite coatings when they are slid against bearing steel ball in the presence of external lubrication. It can be explained by the higher surface roughness of liquid-filled composites. As explained, friction force is dependent on the asperity contacts of the mating surfaces. Higher roughness of the mating surfaces contributes to greater asperity contacts leading to higher COF. As shown in Table 3, the surface roughness (R_a) value of the liquid-filled composites is about 2–3 times greater than those of pure EP or EGN composite coating. Among liquid-filled epoxy composites coating, PFPE-filled composite coating shows higher COF due to its more hydrophilic less oleophilic nature as the PFPE is spread over the top of the coating and lesser bonding with base oil (SN150) is promoted because adhesive forces between two liquids is not as much as the cohesive force. The water contact angle for pure epoxy and epoxy composites were nearly 88° except for EGNPFPE (85°). The oil contact angle for EP and EGNPFPE were nearly 40° whereas for EGN and EGNSN they were 37° and 33° , respectively. Hence, EGN composite coating shows the lowest COF at high (10 N) load because of its higher affinity to externally present base oil (SN150).

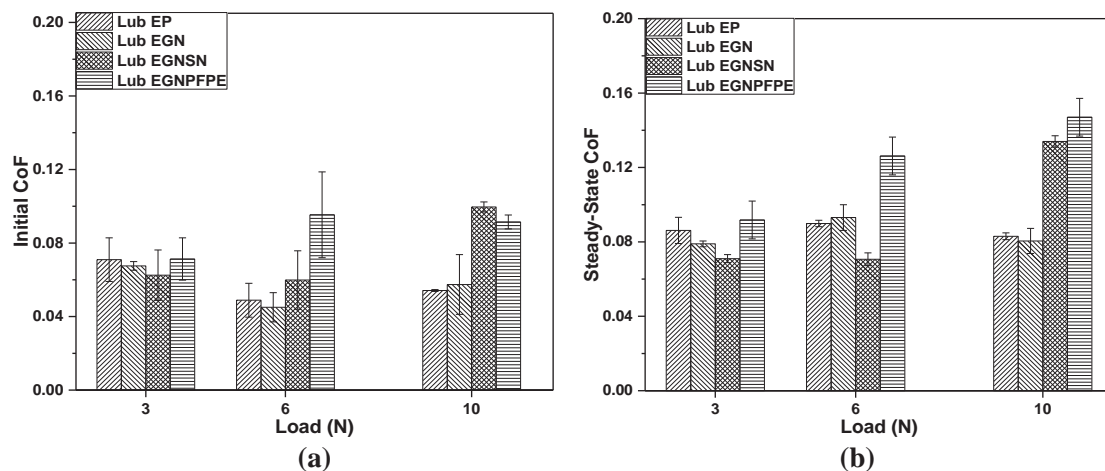


Figure 10. The response of normal load on initial and steady-state CoF for pure EP and composites coated on steel cylinder and tested against a bearing steel ball under base oil lubricated condition. Each filler concentration was 10 wt-%.

Optical microscopy

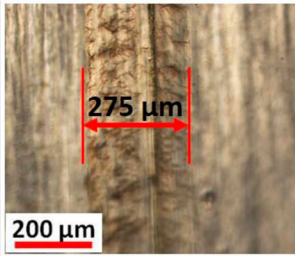
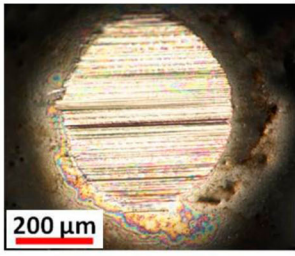
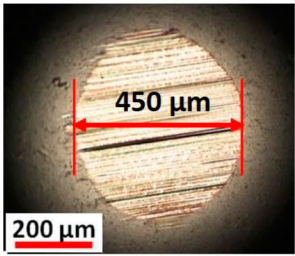
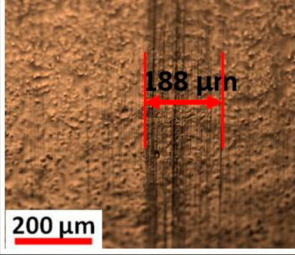
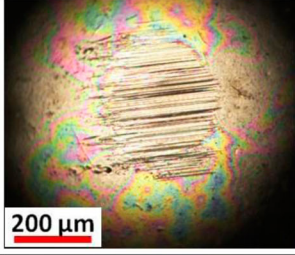
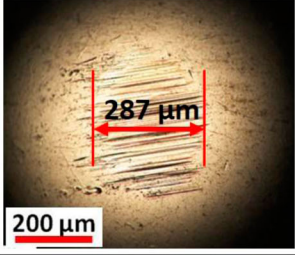
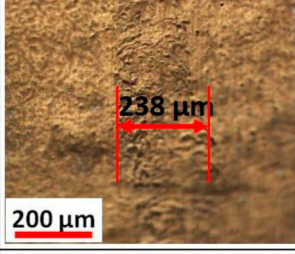
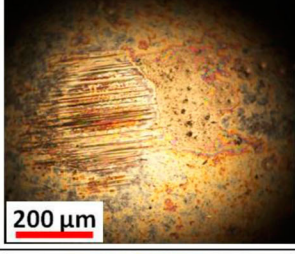
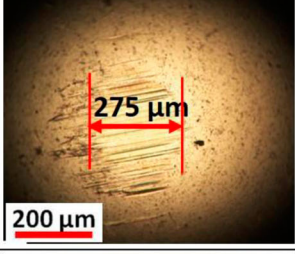
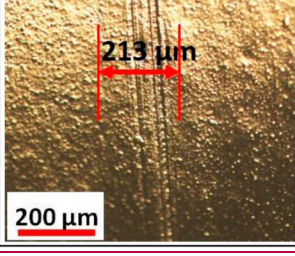
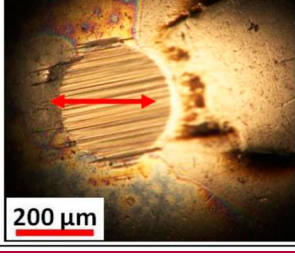
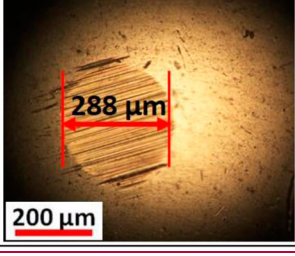
Wear tracks and the corresponding ball images were recorded by Eclipse Confocal Optical Microscope (LV100, Nikon). These images are shown in Table 7 and analysed. The extent of wear on the wear tracks are clearer in the cross-sectional profile as shown in the next section. The wear track for pure epoxy coating is much deeper than those of the composites and is reflected in the measured wear rates. The dimensions on the 'cleaned ball images' show the diameters of the wear scars after the test. It is interesting to note that the steel ball wore most against pure epoxy coating. The reason for this was found to be high wear rate of epoxy and a polishing action of the wear debris. The presence of external liquid lubricant makes it impossible for a protective transfer film to form on the counterface. Hence, wear of a hard surface, such as steel ball, can occur against pure epoxy coating as the wear debris can re-enter the interface along with

the lubricant. Wear of steel ball against the epoxy composites, in comparison, was approximately 36–38% less than that for pure epoxy. Minimum wear of the steel ball counterface was found against the composite EGNNSN. This also reflects the lesser wear of the composites (to be shown in Section 3.5) and hence the amount of wear debris present in the lubricant was minimum. This reduced the wear of the steel ball counterface against epoxy composite by the polishing action.

3D optical profiler analysis

3D optical profiler was used for surface roughness and wear track profile evaluations (Contour GTK, Bruker, USA). The cross-sectional area of the wear track was first calculated by integrating the width and depth profiles (Figure 11). An average of at least ten readings of the cross-sectional area was then multiplied by the

Table 7. The tested specimen images of pure EP, EGN, EGNNSN and EGNPFPE coatings and the corresponding ball images before and after cleaning.

Composites	Worn Surfaces	Ball images after test	Cleaned ball images
Pure Epoxy			
Epoxy/graphene			
Epoxy/graphene/SN1 50			
Epoxy/graphene/PFP E			

The tests were carried out for 200,000 cycles. Wear track width (Column 1) and wear scar diameters (Column 2) are shown by arrows in each image.

circumferential length of the wear track to obtain the wear volume. The specific wear rate (W_{sp}) calculation used the following relation,

$$W_{sp} = \frac{V}{LD} \text{ mm}^3/\text{N} \cdot \text{m},$$

where V is the wear volume, L is the normal load and D is the total sliding distance.

Wear analysis

Wear rates of coatings in externally lubricated sliding condition were measured at 10 N normal load and 0.63 m s^{-1} (300 rev min^{-1}) sliding speed for pure epoxy and the composites. All wear tests were

performed for a fixed (2×10^5) number of cycles. Wear failure of coatings was defined as COF exceeding 0.3, and/or sharp/large fluctuations occurred in the COF readings. Figure 12(a) presents the typical variation of COF with the number of cycles. Figure 12(b) presents the specific wear rate of pure epoxy and epoxy composites at 10 N load and 0.63 m s^{-1} sliding speed under external base oil (SN150) lubricated condition. It is seen in this figure that EP shows much higher wear rate than the composites. The specific wear rate for EP is the highest ($79.3 \times 10^{-7} \text{ mm}^3 \text{ Nm}^{-1}$) under base oil lubricated test. EGNSN composite shows the lowest wear rate ($9.8 \times 10^{-7} \text{ mm}^3 \text{ Nm}^{-1}$) in lubricated test with base oil (SN150). Low wear rate of EGNSN was due to the

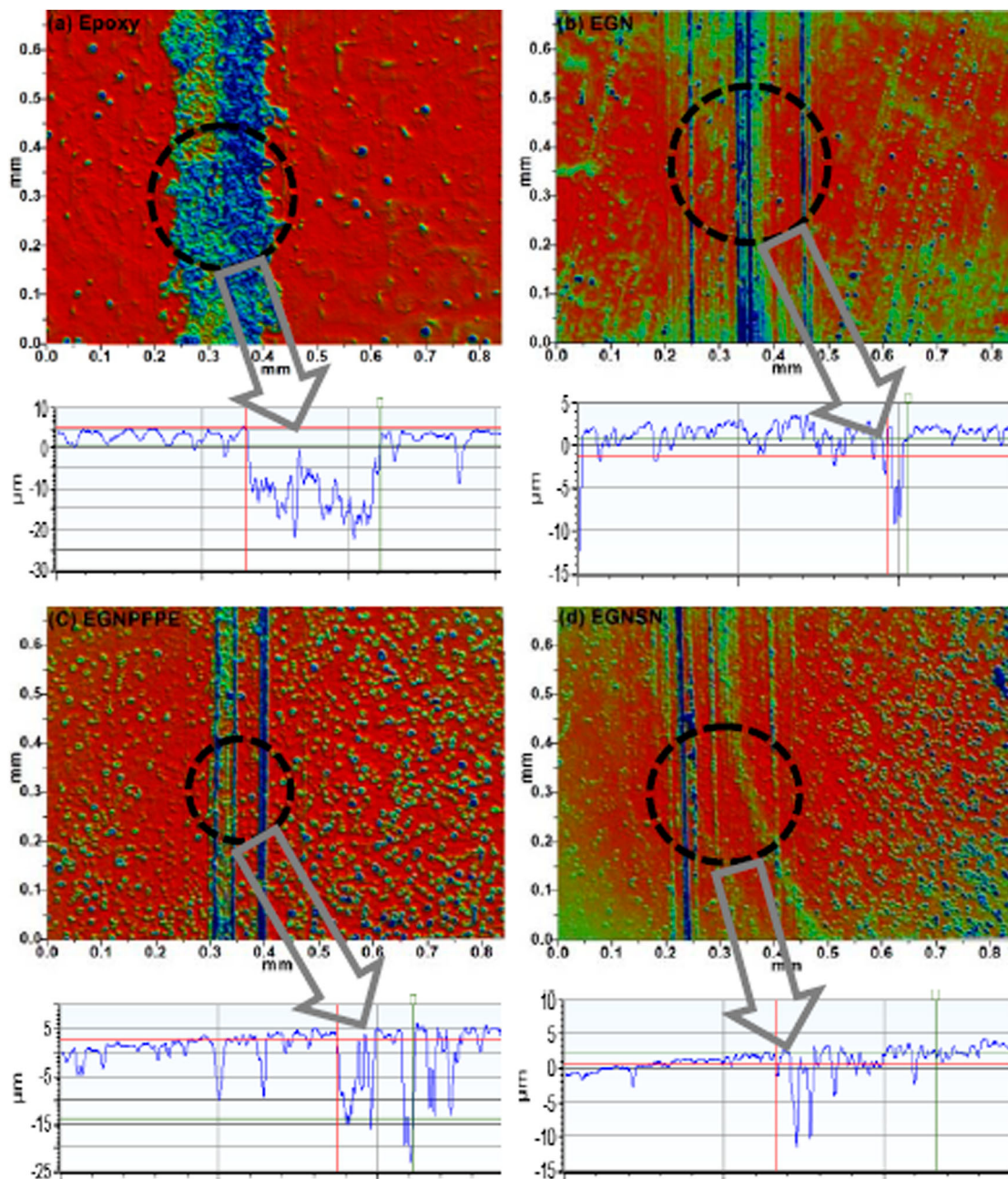


Figure 11. 3D optical profiler images of worn surfaces of epoxy and its composites. The 2D line scans taken across the wear track in the circled part of each image are also included.

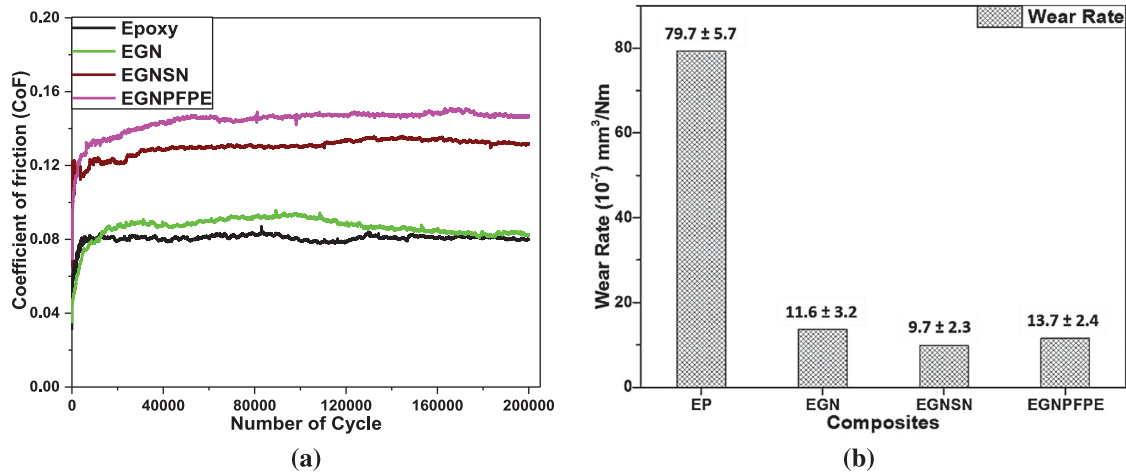


Figure 12. (a) Typical plots of the CoF as a function of the number of cycles for pure epoxy and the composites under external lubrication test condition, and (b) Consolidated specific wear rate data for EP and the composites after complete run of 200,000 cycles of sliding under externally lubricated condition. The tests were conducted at the speed of 0.63 m s^{-1} (300 rev min^{-1}) and normal load of 10 N.

presence of lower contact area as compared to EP and other composites as it had higher roughness value as compared to others. Although, we observed that higher roughness gave higher CoF for EGNSN150 and EGNPFPE composites, in terms of wear resistance, it had beneficial effects. Wear rate performance of EGNS150 was best when compared with only graphene or graphene/PFPE composites. Thus, the results showed that *in situ* lubricated composites of EGN provided a practical tribological solution of low friction in mixed lubrication regime with low wear rate. All of the composite coatings survived beyond 200,000 cycle of sliding (experiments were terminated at 200,000 sliding cycles) at the maximum normal load of 10 N used in this study.

Conclusions

Pure epoxy and its composites (10 wt-% of graphene) filled with liquid lubricants (10 wt-% of SN150 or PFPE) coated on D2 steel substrate were tested in base oil externally lubricated sliding condition at different loads and sliding speeds to evaluate their tribological performances against a counterface of 4 mm steel (SAE 52100) ball. Mechanical, thermal and surface property characterisations were carried out. Wear tests were conducted for 200,000 sliding cycles. The following conclusions are drawn:

- (i) The coefficients of friction of epoxy composite coatings on D2 steel reduced under base oil lubricated condition with low wear rate (more than two times reduction in the CoF over the sample in dry sliding condition).
- (ii) With external lubrication, the CoF for EGN (epoxy filled with graphene) composite is the lowest (~ 0.04 – 0.08) among all composites and nearly constant at all sliding speeds. The lubrication

mechanism is mixed lubrication and follows the Briscoe and Evan's linear relation between shear stress and logarithm of sliding speed.

- (iii) The wear rate for EGNSN (epoxy/graphene/SN150) with external lubrication is the least at $9.8 \times 10^{-7} \text{ mm}^3 \text{ Nm}^{-1}$ at 10 N load. The composite EGN (epoxy/graphene) gives slightly higher wear rate of $11.6 \times 10^{-7} \text{ mm}^3 \text{ Nm}^{-1}$ at the same load.

Acknowledgements

The provision of research facilities and internal grants by IIT Kanpur and IIT Delhi is gratefully acknowledged by the authors.

Disclosure statement

No potential conflict of interest was reported by the authors.

References

- [1] Vizintin J, Kalin M, Dohda K, et al. Tribology of mechanical systems: a guide to present and future technologies. New York: American Society of Mechanical Engineers; 2004.
- [2] Gold PW, Loos J. Wear resistance of PVD coatings in roller bearings. *Wear*. 2002;253:465–472.
- [3] Erdemir A, Nichols FA, Pan XY. Friction and wear performance of ion-beam-deposited diamond-like carbon films on steel substrates. *Diam Relat Mater*. 1994;3:119–125.
- [4] Grill A. Tribology of diamond like carbon and related materials: an updated review. *Surf Coat Technol*. 1997;94–95:507–513.
- [5] Gahlin R, Larsson M, Hedenqvist P. ME-C:H coatings in roller bearings. *Wear*. 2001;249:302–309.
- [6] Siu JHW, Li LKY. An investigation of the effect of surface roughness and coating thickness on the friction and wear behavior of a commercial MoS₂-metal coating on AISI 400C steel. *Wear*. 2000;237:283–287.

- [7] Neville A, Morina A, Haque T, et al. Compatibility between tribological surfaces and lubricant additives – how friction and wear reduction can be controlled by surface/lube synergies. *Tribol Int.* **2007**;40:1680–1695.
- [8] Li J, Ren T, Liu H, et al. The tribological study of a tetrazole derivative as additive in liquid paraffin. *Wear.* **2000**;246:130–133.
- [9] Suh NP. *Tribophysics*. Englewood Cliffs (NJ): Prentice-Hall; **1986**.
- [10] Samad MA, Satyanarayana N, Sinha SK. Tribology of UHMWPE film on air-plasma treated tool steel and effect of PFPE overcoat. *Surf Coat Technol.* **2010**;204:1330–1338.
- [11] Kumar V, Sinha SK, Agarwal AK. Tribological studies of epoxy and its composite coatings on steel in dry and lubricated sliding. *Tribol-Mater surf Interface.* **2015**;9:144–153.
- [12] Shah R, Datashvili T, Cai T, et al. Effects of functionalised reduced graphene oxide on frictional and wear properties of epoxy resin. *Mater Res Innov.* **2015**;19(2):97–106.
- [13] Wan YZ, Luo HL, Wang YL, et al. Friction and wear behavior of three-dimensional braided carbon fibre/epoxy composites under lubricated sliding conditions. *J Mater Sci.* **2005**;40(17):4475–4481.
- [14] Saravanan P, Sinha SK, Jayaraman S, et al. A comprehensive study on the self-lubrication mechanism of SU-8 composites. *Tribol Int.* **2016**;95:391–405.
- [15] Kumar V, Sinha SK, Agarwal AK. Tribological studies of epoxy composites with solid and liquid fillers. *Tribol Int.* **2017**;105:27–36.
- [16] Tabor D. Mechanism of boundary lubrication. *Proc R Soc Lond A Math Phys Sci.* **1952**;212:498–505.
- [17] Gelinck ERM, Schipper DJ. Calculation of Stribeck curves for line contacts. *Tribol Int.* **2000**;33:175–181.
- [18] Lu L, Khonsari MM, Gelinck ERM. The Stribeck curve: experimental results and theoretical prediction. *J Tribol.* **2006**;128:789–794.
- [19] Briscoe BJ, Evans DCB. The shear properties of Langmuir–Blodgett layers. *Proc R Soc Lond A.* **1982**;380:389–407.